ADVANCES IN ATMOSPHERIC SCIENCES, VOL. 24, NO. 3, 2007, 409–420

Moisture Analysis of a Squall Line Case Based on Precipitable Water Vapor Data from a Ground-Based GPS Network in the Yangtze River Delta

DING Jincai*[1,2] (丁金才), YANG Yinming[2] (杨引明), YE Qixin[2] (叶其欣), HUANG Yan[1] (黄 炎), MA Xiaoxing[1] (马晓星), MA Leiming[3] (马雷鸣), and Y. R. GUO[4]

[1] *Shanghai Meteorological Center, Shanghai* 200030

[2] *Shanghai Remote Sensing and Measurement Application Center*

[3] *Shanghai Typhoon Institute, Shanghai* 200030

[4] *National Center for Atmospheric Research, CO, USA*

(Received 20 March 2005; revised 6 September 2006)

ABSTRACT

A squall line swept eastward across the area of the Yangtze River Delta and produced gusty winds and heavy rain from the afternoon to the evening of 24 August 2002. In this paper, the roles of moisture in the genesis and development of the squall line were studied. Based on the precipitable water vapor (PWV) data from a ground-based GPS network over the Yangtze River Delta in China, plus data from a Pennsylvania State University/National Atmospheric Center (PSU/NCAR) mesoscale model (MM5) simulation, initialized by three-dimensional variational (3D-VAR) assimilation of the PWV data, some interesting features are revealed. During the 12 hours prior to the squall line arriving in the Shanghai area, a significant increase in PWV indicates a favorable moist environment for a squall line to develop. The vertical profile of the moisture illustrates that it mainly increased in the middle levels of the troposphere, and not at the surface. Temporal variation in PWV is a better precursor for squall line development than other surface meteorological parameters. The characteristics of the horizontal distribution of PWV not only indicated a favorable moist environment, but also evolved a cyclonic wind field for a squall line genesis and development. The "+2 mm" contours of the three-hourly PWV variation can be used successfully to predict the location of the squall line two hours later.

Key words: squall line, global positioning system (GPS), precipitable water vapor (PWV)

DOI: 10.1007/s00376-007-0409-y

1. Introduction

A squall line is a narrow and active thunderstorm belt, often producing severe weather events. Generally, a squall line extends for hundreds of kilometers in length and tens of kilometers in width. When a squall line arrives, surface meteorological parameters change suddenly, with the subsequent strong gales and heavy rain often causing serious damage and disaster over a short period of time (Zhang et al., 2001; Shou, 2002). Because squall lines possess the characteristics of a short lifespan, plus a small horizontal scale and fast movement, it is difficult to analyze and forecast them using conventional observation data. From the afternoon to the evening of 24 August 2002, a squall line swept across the area of the Yangtze River Delta. When it arrived in the Shanghai area at 2018 LST, the surface meteorological parameters changed rapidly, as shown in Fig. 1. Within one hour, the temperature had cooled to 8.5°C, pressure had risen to 3.7 hPa, and absolute humidity had increased to 4.0 g m^{-3}. In the surface chart at 2000 LST a narrow zone of northwest gales with a mean wind speed of 8–14 m s^{-1} existed. Maximum gusts reached 29 m s^{-1} in Fengxian County,

*E-mail: dingjincai@hotmail.com

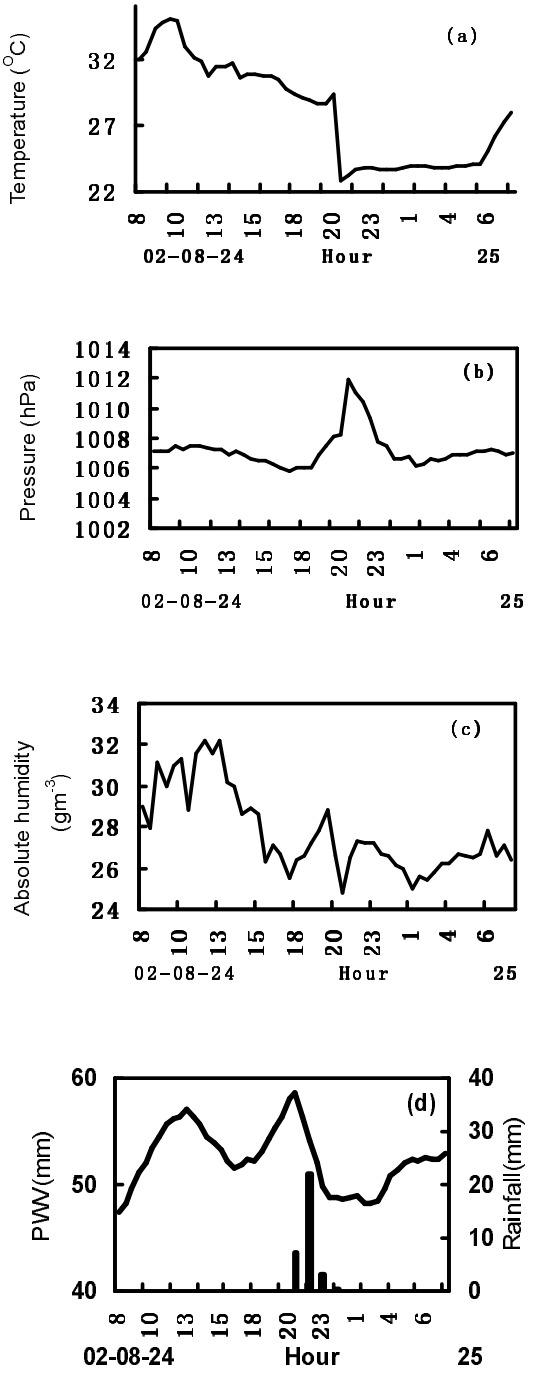

Fig. 1. Variation in the surface meteorological elements of (a) temperature, (b) pressure, (c) absolute humidity, and (d) PWV and hourly rainfall in Pudong station in Shanghai during the squall line process. In (d), the magnitude of PWV variation is denoted by the left ordinate, and vertical columns represent the hourly rainfall, for which magnitude is denoted by the right ordinate.

Shanghai, and the maximum hourly rainfall was 57 mm. However, one hour later, after the squall line had passed the Shanghai area, pressure and absolute humidity decreased immediately and then returned to normal levels in the following three hours. These phenomena confirm a typical squall line.

Qi and Chen (2004) analyzed the genesis and development of a squall line based on data from conventional synoptic charts, satellite images and Doppler radar observations. The present paper focuses on the effects of moisture on the genesis and development of a squall line, and is based on the precipitable water vapor (PWV) data from a ground-based GPS network in the Yangtze River Delta, China, as well as data from a mesoscale numerical model (MM5) simulation, initiated by three-dimensional variation (3D-Var) assimilating the GPS/PWV data. The MM5 model was introduced in detail by Grell et al. (1993) and Dudhia et al. (1995). Some efforts are being made to discover the signals useful for predicting the movement and development of squall lines.

2. The ground-based GPS network in the Yangtze River Delta and PWV measurement

As part of an effort to enhance water vapor measurement in an attempt to improve weather forecasting, a ground-based GPS network was established in June 2002 in the Yangtze River Delta, China. It covers the area of 29.5°–33.0°N and 118.0°–122.0°E, and consists of 14 fiducial GPS stations. The distances between the stations are around 23 km within the Shanghai area and 107 km outside (Fig. 2). The GPS net-

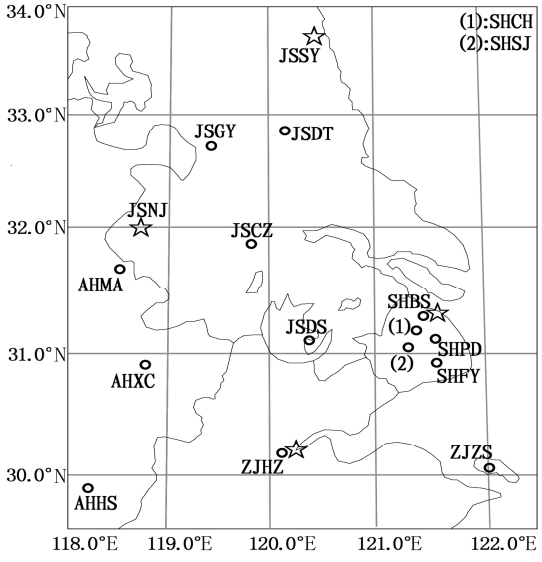

Fig. 2. GPS network in the Yangtze River Delta, China. The symbol ∘ indicates the GPS stations, and ★ the radiosonde stations. The stations' names are indicated by the four capital letters.

work provides PWV data every 30 minutes in real time. PWV is the total water vapor in an air column. Generally, PWV can be expressed as the height of the equivalent liquid column, in units of mm (The Meteorological Speciality of the Geophysical Department of Beijing University, 1976):

$$q = \sum \omega_i = \sum e_i \times \Delta h_i \ . \tag{1}$$

Here, e_i is the absolute humidity at a given layer, Δh_i is the thickness of the layer, ω_i is the moisture content in the layer, and i indicates the list number of the layer from the ground.

The technique of measuring GPS-PWV was advanced by, among others, Bevis et al. (1992), Bevis et al. (1994), and Businger et al. (1996). GPS microwave frequency signals are delayed by the ionosphere and neutral atmosphere. The delay in the ionosphere is approximately proportional to the inverse square of the signal frequency, and can be eliminated using the duel-frequency technique. The total zenith neutral delay (ΔL) consists of two parts: wet delay ($\Delta L_{\rm w}$), caused by moisture and hydrostatic delay, or dry delay ($\Delta L_{\rm h}$), caused by the other part of the atmosphere. The zenith dry delay can be estimated precisely based on the surface pressure. Then the zenith wet delay is obtained by subtracting the dry delay from the total zenith delay. The differential estimated zenith delay can be written as:

$$\Delta L = \Delta L_{\rm h} + \Delta L_{\rm w} \ , \tag{2}$$

$$\Delta L_{\rm h} = (2.2768 + 0.0005) p_0 / f(\lambda, H) \ , \tag{3}$$

where $\Delta L_{\rm h}$ and $\Delta L_{\rm w}$ are dry delay and wet delay, respectively, both in mm, and p_0 is the surface pressure in hPa.

$$f(\lambda, H) = 1 - 0.00266 \cos 2\lambda - 0.00028 H \ , \tag{4}$$

where λ is the latitude and H is the station's altitude in meters.

The relationship between q and $\Delta L_{\rm w}$ can be expressed as follows:

$$q = \Pi \times \Delta L_{\rm w} \ , \tag{5}$$

where Π is a conversion factor.

$$\Pi = 10^6 [R_{\rm w} \times (k_2' + k_3 T_{\rm m}^{-1})]^{-1} \ , \tag{6}$$

where $R_{\rm w}$=461.495 J kg^{-1} K^{-1}, and is the specific gas constant for water vapor, $k_2' = 22$ K hPa^{-1}, and $k_3 = 377600$ K^2 hPa^{-1} are physical constants. $T_{\rm m}$ is the weighted mean temperature of the wet part of the atmosphere, which can be estimated by an experimental function of surface temperature, $T_{\rm s}$, as:

$$T_{\rm m} = 70.2 + 0.72 T_{\rm s} \ . \tag{7}$$

Comparing real time PWV data from the GPS network (GPS-PWV) with PWV derived at the nearest radiosonde stations (RADIO-PWV) for the period June 2002–December 2003, it is found that the root of mean square (RMS) of the error is 3.1 mm with a relative error of 7.09%, and the correlation coefficient between them reached 0.96. This, to a certain extent, shows the GPS-PWV data to be of good quality.

3. Description of the squall line event

Based on an analysis of conventional weather charts and satellite cloud images, Qi and Chen (2004) studied a squall line formed in a mesoscale convective system (MCS). The southwest current along the northwest edge of the subtropical high brought abundant moisture to the east part of China, and a convergence line laid in the Yangtze River Delta. Besides, there existed instable stratification. All of the conditions helped the thunderstorms in the MCS develop to become a squall line. The squall line produced heavy rain, and the front of the rain area corresponded to the movement and development of the squall line. Figure 3 shows the evolution of hourly rainfall area in the Yangtze River Delta during the squall line event. Herewith, we explain several of the hourly rainfall charts due to space limitations within the paper. At 1400 LST, one hour prior to the squall line being formed, no precipitation occurred in the whole of the Yangtze River Delta. At 1500 LST (Fig. 3a), the squall line formed and produced a rain area; the maximum hourly rainfall was 24 mm. As the squall line moved eastward, the rain area also moved eastward and intensified. At 1800 LST (Fig. 3c), the rain area extended eastward across 120oE and continued to intensify, becoming heavy rain with a maximum of over 30 mm of hourly rainfall. At 2000 LST (Fig. 3d), the rain area approached the west of Shanghai and intensified further with a maximum of 41 mm per hour. When the squall line influenced the Shanghai area at 2100 LST, the surface meteorological parameters changed suddenly at Pudong station, as shown in Fig. 1. The precipitation covered the entire area of Shanghai, and in about one third of the Shanghai area the rainfall rate exceeded 30 mm per hour, with the maximum of 57 mm observed in Fengxian County (Fig. 3e). One hour later, as the squall line moved away from the Shanghai area, the rain area began to move into the East Sea and the intensity began to weaken. Combining the analysis of radar data and surface meteorological data, the front edge of the rainfall isoline of 1 mm coincided roughly with the location of the squall line (see Fig. 3).

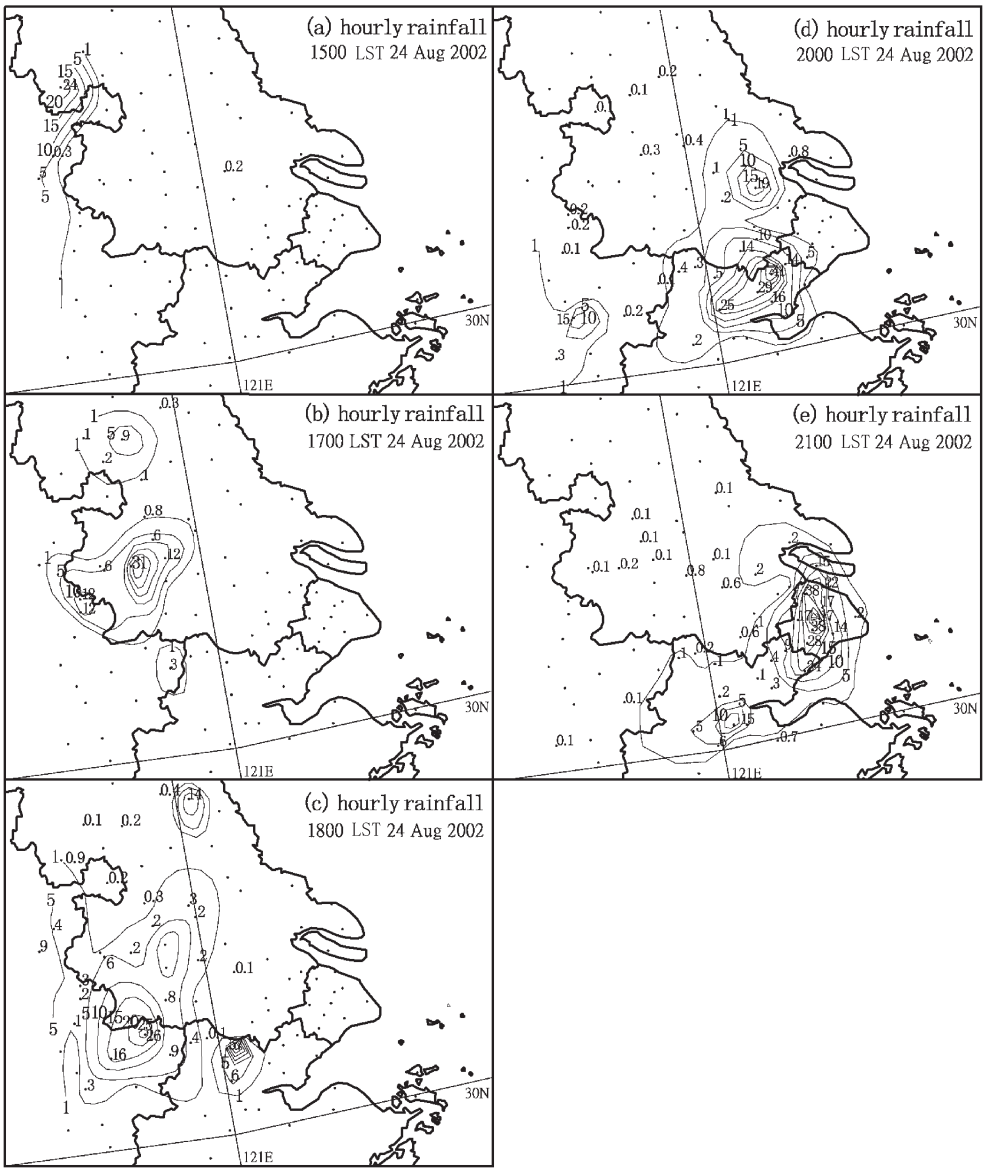

Fig. 3. Evolution of hourly rainfall area in the Yangtze River Delta during the squall line event. Rainfall is in mm.

4. Temporal variation of PWV at Pudong station in Shanghai (SHPD)

The squall line produced heavy rains when it was moving eastward, for which continuous moisture supply was a necessary condition. Figure 1d shows the temporal variation of PWV at SHPD station, Shanghai. Twelve hours prior to the arrival of the squall line, there were two stages of significant increase in PWV. First, PWV increased from a low of 47.4 mm at 0800 LST, before exceeding 50 mm at 0930 LST. Based on the recent statistical results 50 mm of PWV is a tolerance to alarm occurrence of a precipitation process in this season. PWV increased continuously and reached its first peak of 57.0 mm at 1330 LST. This implies that moisture in the air had been enough for precipitation generation, but the deficiency was the dynamical conditions, convergence and updraft, which could be diagnosed from the surface and 850 hPa synoptic charts. After a short and small decline from 1400 to 1630 LST, PWV began its second stage of increase and reached a maximum of 57.7 mm in the day. The two stages of PWV increase demonstrates that moisture existed sufficiently for the squall line to produce such heavy rain. Actually, at the stations along the route of the squall line movement, such as Ma'anshan station in Anhui Province (AHMA), Changzhou station and Dongshan station in Jiangsu Province (JSCZ

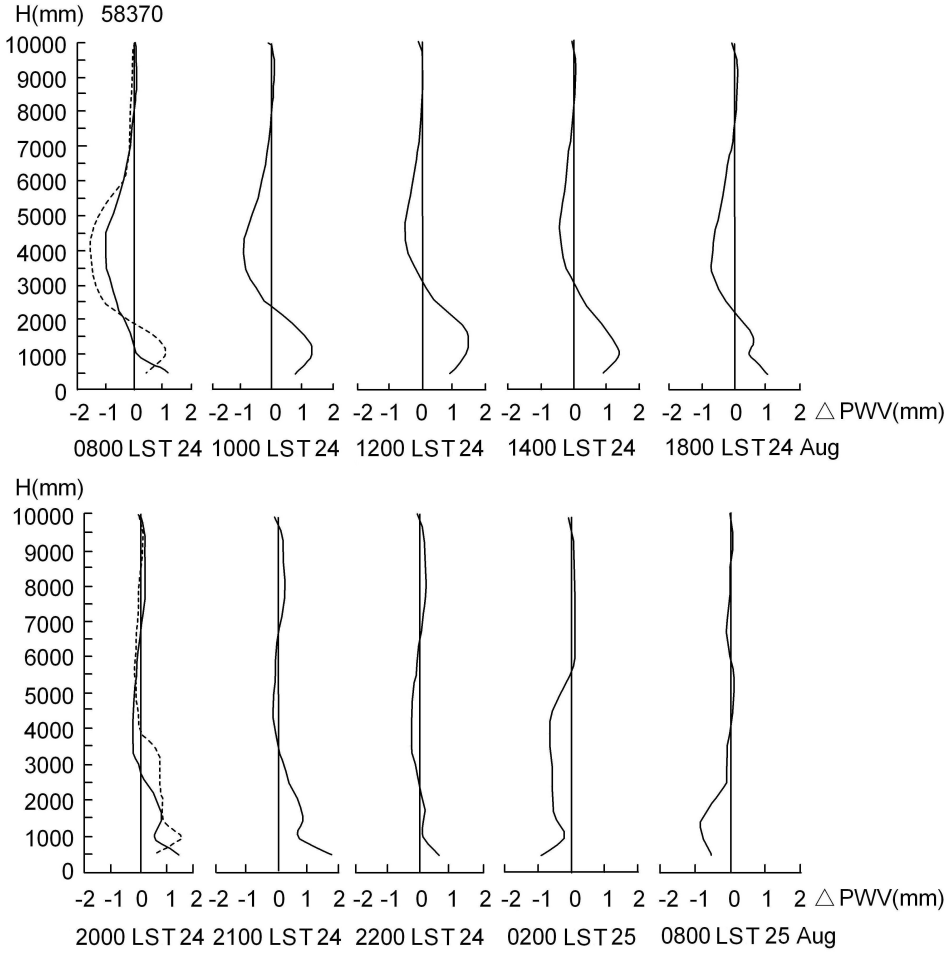

Fig. 4. Evolution of the moisture anomaly profile at SHPD station from 0800 LST 24 August 2002 to 0800 LST 25 August 2002. The abscissa denotes the anomaly of ω_i in mm; the ordinate is the height in m. The solid line shows the moisture anomaly profile of adjusted ω_i. The dashed lines at 0800 and 2000 LST 24 August 2002 are the moisture anomaly profiles from the radiosonde data.

and JSDS), the PWV showed a similar pattern of increase over a different time (figures not shown here). The continuous increase of PWV for several hours prior to the arrival of the squall line is a necessary condition for heavy rain.

As shown in Figs. 1a–c, the surface meteorological parameters did not show any significant variation prior to the arrival of the squall line. They changed suddenly only at the time when the squall line had arrived. On the contrary, the surface absolute humidity decreased continuously from 1400 LST, and, although it increased by around 3 g m^{-3} from 1700 to 2000 LST, the peak value was much lower than before 1400 LST. Furthermore, at 2100 LST the absolute humidity decreased suddenly to its lowest point for the day. At that time, the squall line happed to influence the whole of the Shanghai area (see Fig. 3e) and PWV increased to its peak for the day (Fig. 1d). It is revealed that before the arrival of the squall line, moisture increased significantly in the layers above the surface, but not at the surface. Thus, real time PWV data with a high temporal resolution can reflect the approach of a squall line better than surface meteorological parameters.

In order to further analyze the impact of the evolution of the moisture profile on the squall line, the hourly vertical profile of the moisture content with a vertical interval of 500 m was retrieved: namely, ω_i. Generally, the three dimensional moisture distribution based on water vapor data from a ground-based GPS network can be retrieved by two methods. The first is called GPS water vapor tomography, and this method requires a ground-based GPS network with a high resolution. MacDonald and Xie (2002) suggested that if there are approximately 100 observations within one hour per GPS station and if the retrieved three dimensional moisture is required with vertical revolu-

tion of 500 m, the ground-based GPS station network should be formulated with 40 km resolution. Bi (2006) pointed out that the quality of moisture data in a three dimensional distribution retrieved by tomography is related closely to the horizontal distances between GPS stations. If the cut-off elevation angle of the GPS station is 15°, the mean distance between GPS stations should be within 50 km. As the mean distance between GPS stations in the Yangtze River Delta is 107 km, thus it is difficult to get good enough three-dimensional moisture distributions using tomography based on the GPS network. Herewith, the other method of the MM5 forecasted moisture field adjusted by observed GPS-PWV is adopted.

Yuan et al. (2004a) compared hourly PWVs forecasted by MM5 with those retrieved by a GPS network. The RMS between them was 4.03–4.6 mm and the correlation coefficient between them reached 0.90–0.96 in a 24-hour forecasting period. The errors of forecasted PWVs remained small and stable within 19 hours, then increased obviously with forecast time (figure omitted). It has been certified that 3D-VAR assimilation with PWV data from a GPS network can improve the MM5 initialization and forecasts of the moisture field (Kuo et al., 1993; Kuo et al., 1996; MacDonald and Xie, 2002; Yuan et al., 2004b). Besides, the hourly moisture field can be better simulated if the forecasted moisture field of MM5 is corrected by hourly observed PWV from the GPS network. This is the reason that the second method is adopted here instead of tomography. The procedure of the second method is as follows:

First, the observed PWV data at 0800 LST 24 August 2002 in the Yangtze River Delta are assimilated with 3D-VAR to obtain the initial field of the MM5 model. The model resolution is 15 km with 27 vertical levels, and its moisture physical processes adopts the parameterization scheme of the mix phase including ice; the cumulus parameterization adopts the Betts-Miller(BM) scheme (Betts, 1986; Betts and Miller, 1986; Betts and Miller, 1993). The integral time step is 120 seconds. Then, the hourly absolute humidity forecasts at every iso-pressure level are interpolated to the height levels with an interval of 500 m by the exponential lapse rate. Thirdly, the hourly forecasted moisture content at each level, and the PWV at each station are calculated as ω_{fi} and $q_{\rm f}$, respectively. Comparing with the hourly observed PWV ($q_{\rm o}$) at SHPD station from 0800 LST 24 August to 0200 LST 25 August, the RMS of the error of forecasted $q_{\rm f}$ with assimilation of PWV data is 0.45 mm. This is 7.4% smaller than without assimilation of PWV. Therefore, the forecasted $q_{\rm f}$ with 3D-Var assimilation is taken for further analysis. Finally, the forecasted moisture content $\omega_{\rm fi}$ at each level was adjusted by the observed $q_{\rm o}$ according to the following formula (Kuo et al., 1993; Kuo et al., 1996; Yuan et al., 2004b):

$$\omega_i = \omega_{fi} + (q_{\rm o} - q_{\rm f}) \times \omega_i / q_{\rm f} \,. \tag{8}$$

ω_{fi} means forecasted moisture content at each level, which is adjusted by the observed $q_{\rm o}$ and forecasted $q_{\rm f}$. The ω_i has an additional restriction condition than that of the non-adjusted $q_{\rm f}$, in that it kept the total sum of ω_i equal to the observed $q_{\rm o}$. This constraining condition made the ω_i to be closer to the real moisture profile. Figure 4 illustrates the evolution of the moisture anomaly profile. The anomaly is defined as the difference of the ω_i at a certain time minus the monthly mean of the corresponding ω_i from the radiosonde data in August 2002.

In Fig. 4 the dashed lines at 0800 and 2000 LST 24 August 2002 show the moisture anomaly profile from radiosonding data. At the higher levels above 4000 m, the ω_i profiles from the radiosonde data coincided well with the adjusted ω_i. At the lower levels, both the ω_i anomalies have the same anomaly sign, although the observed ω_i anomalies from the radiosonde data are larger than the adjusted ω_i anomalies. The temporal evolution of their moisture profile retained a reasonable continuity. So, the profiles of the adjusted ω_i anomaly in Fig. 4 can basically be taken as the real moisture fields to analyze the evolution of the moisture profile. From 0800 to 1200 LST, the moisture profile showed a positive anomaly at the lower levels under 2000 m and a negative anomaly at the middle levels between 2000 m and 7000 m; the maximum of the negative anomaly located at a height of 4000 m. These characteristics of the moisture profile—more moist at the lower levels and dryer at the middle levels—made the potential pseudo-equivalent temperature ($\theta_{\rm se}$) decrease with height, and formed an unstable stratification. It led the moisture to transfer from lower levels to upper levels; from 0800 to 1400 LST the top of the wet low layer increased from 1500 m to 3000 m high. Meanwhile, the negative anomaly in the middle levels were decreasing. This led to the first stage of PWV increase. From 1800 LST, although the positive ω_i anomaly at the lower levels reduced, the negative ω_i anomaly in the middle levels reduced more obviously and turned to be near zero. This indicates the total moisture in the atmosphere should increase from 1800 LST, to supply sufficient moisture for the squall line development as it approached. As the squall line moved eastward out of the Shanghai area, the vertical distribution of moisture became contrary. From 2200 LST, the ω_i anomaly below 3000 m began to change to negative, and up until 0200 LST 25 August, the ω_i anomaly turned to negative below 6000 m and to posi-

tive above 6000 m, making the atmospheric stratification dry and stable. This led to PWV falling rapidly after the squall line had passed the Shanghai area, as shown in Fig. 1d.

The evolutionary characteristics of the moisture profile related closely to the evolution of the wind profile. Figure 5 illustrates the evolution of wind profiles from a wind profiler at Qingpu station in Shanghai (quoted from Qi and Chen, 2004). This is a boundary level wind profiler, and the top of the wind sounding is near to 2500 m high. At the lower levels, under 800 m, southwest winds prevailed from 0800 to 1200 LST, which was favorable for moisture to be transported into the Shanghai area and caused the lower layer to become wet. This made the absolute moisture at the surface increase significantly from 0800 to 1400 LST, as shown in Fig. 1c. The significant positive moisture (ω_i) anomaly existed in the lower layer. The maximum of the positive ω_i anomaly was at a height of 1000–1500 m. The positive ω_i anomaly at this height was increasing with the time, and it reached a maximum of 1.52 mm at 1300 LST and 1.47 mm at 1400 LST, increasing by 1.47 mm and 1.26 mm more than the positive ω_i anomaly at 0800 LST at that level. Actually, in the whole of the lower layer of 500–2500 m, the sum of the positive ω_i anomaly at 1400 LST increased by 4.58 mm more than that at 0800 LST. On the contrary, at the levels above 800 m, the northwest wind prevailed from 0800 to 1200 LST. The radiosonding at 0800 LST observed northwest winds with 10–14 m s^{-1} from 3000–5000 m. The 700 hPa and 500 hPa weather charts at 0800 LST 24 August showed the Shanghai area was influenced by the northwest winds in the front of a weak high ridge (figure omitted). It proved a dry and cold air current in the middle levels penetrated over the Shanghai area and led to the negative moisture anomaly in the middle layer from 2000–6000 m high. The most significant negative ω_i anomaly was at a height of 4000–4500 m. As the wind speeds were decreasing and the wind directions were backing with time, the absolute value of the negative ω_i anomaly was reducing too. The sum of the moisture anomaly in the middle layer of 3000–6000 m at 1400 LST increased by 0.65 mm. This reveals that in the first stage of PWV increase from 0800 to 1400 LST, moisture at all levels increased, but moisture in the lower levels increased more than that in the middle levels. It is worth noting that convection played an important role in moisture increase. This kind of wind profile during the first stage formed an unstable atmospheric stratification, with dry air in the middle layer and wet air in the lower layer, which was favorable for convection to develop and bring moisture up. The top of the lower wet layer was increasing to 2500–3000 m high, as shown in Fig. 4. Meanwhile, the southwest current under 800 m supported the moisture supply. This resulted in the increase in thickness of the lower wet layer and the main part of the PWV increase.

From 1400 LST the wind profile changed. The wind direction under 800 m changed to northeast and then to northwest between 2000 and 2200 LST. The moisture supply became weak, which resulted in the absolute moisture at the surface decreasing significantly from 1400 LST, as shown in Fig. 1c. The positive moisture anomaly under 2500 m was reducing with time and reached a minimum at 1800 LST. Although the moisture anomaly began to increase again from 1800, the sum of the moisture anomaly increase in the lower layer of 500–2500 m at 2100 LST increased by only 1.53 mm more than that at 1800 LST. Meanwhile, the wind direction above 2000 m high changed to southwest or west. The 700 hPa and 500 hPa weather charts at 2000 LST showed a weak ridge just moving into the sea. A southwest current existed over the Shanghai area and brought moisture to the middle levels. This led to the negative moisture anomaly in the middle levels beginning to reduce. The wind speeds over 200 m increased rapidly from 1800 LST and led to the moisture anomaly in the middle levels tending to zero. The sum of the moisture anomaly in the middle layer of 3000–6000 m at 2100 LST increased by 3.24 mm more than that at 1800 LST. Comparing with the moisture increase of 1.53 mm in the lower layer, it is obvious that the PWV increase in the second stage was mainly due to the moisture increase in the middle levels.

5. Evolution of the spatial distribution of PWV

Figure 6 illustrates the evolution of the PWV spatial distribution when the squall line formed and moved into the Yangtze River Delta. From 0800 to 1300 LST (Figs. 6a and 6b), the PWV values in the northern part of the area maintained higher than 52 mm, and a moisture convergence existed in this part of the area due to the moisture current from the northwest side of the subtropical high. Meanwhile, a dry trough marked by lower PWV existed from the northeast to the southwest in the southern part of Yangtze River Delta. This distribution of PWV changed little during this period. At 1400 LST (Fig. 6c), the PWV along the border of Jiangsu and Anhui Provinces increased suddenly, and so the PWV at station AHMA increased by 6.5 mm and reached 58.4 mm during the last three hours, and the PWV at station AHXC and JSCZ increased by 1.7 mm and 1.6 mm, respectively. This indicates that moisture increased rapidly in that

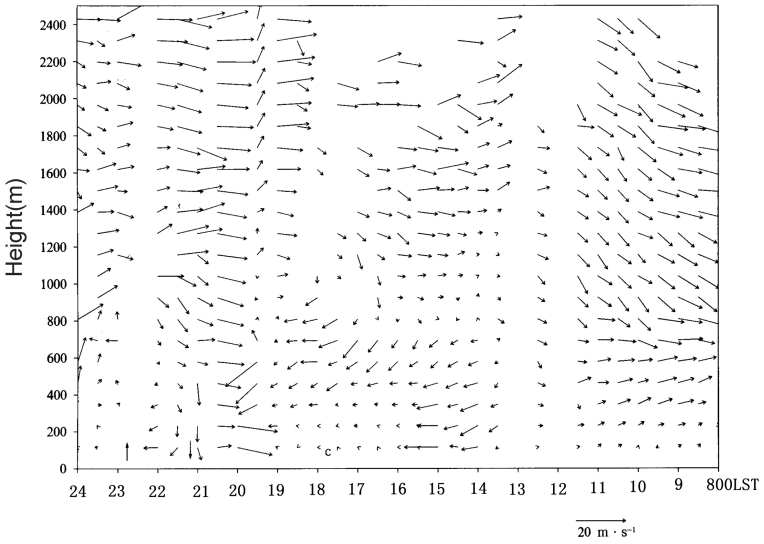

Fig. 5. Evolution of the wind profiles from 0800 to 2400 LST 24 August 2006 observed at the Qingpu station in Shanghai. Unit of wind speed is indicated in the bottom right.

area. One hour later the squall line formed and produced a rain area with a maximum hourly rainfall of 24 mm. This proved the rapid increase of moisture in the air played an important role in the outgrowth of a squall line. From 1500 to 1700 LST (Fig. 6d), the area of high PWV expanded southeastward, and the PWV in the whole northern part of the Yangtze River Delta increased continuously and significantly. The PWV at station JSDS at 1700 LST increased by 4.7 mm during the last three hours. At 1700 LST, however, the squall line was located west to 120°E, and two hours later it arrived at station JSDS. A similar situation occurred at station AHMA, with the PWV rapidly increasing ahead of the arrival of the squall line for 1–2 hours. This variation provides a sign to predict the movement and development of a squall line. The PWV distribution at 0900 LST (Fig. 6e) is opposite to the earlier situation, with higher PWV in the east part and lower PWV in the west part of the Yangtze River Delta. PWV in the Shanghai area and the northern part of Zhejiang Province exceeded 53 mm, meanwhile the dry trough disappeared. The squall line arrived in the Shanghai area and produced very heavy rains in two hours.

In order to determine an exact relationship between the variation of PWV and the location of the squall line, we plotted the three-hour PWV variations overlapped by the contours of 1 mm of hourly rainfall two hours later. According to the statistical results of the PWV variation in intervals of one-hour, two- hours, three-hours and up to six- hours at several GPS stations in the path of te squall line, the three-hour PWV variations are much more significant than one-hour and two-hours variation, while the 4-hours up to six-hours variations change very little and even less than the three-hours variation. It indicates that the three-hour PWV variations (written as $\Delta_3 q$) is most suitable to present the PWV variations in the squall line case. The mean RMS values show the variations of PWV increased rapidly from one hour to three hours, while it increased at a much smaller rate in the following three hours. The maximum of the PWV variation occurred in three hours at all stations except SHPD. Besides, the life of the squall line was only seven to eight hours; the six-hour variation of PWV seemed too long to express the influence of the squall line.

Figures 7a–f show these plots at 1400 to 1900 LST. The solid lines are the contours of positive $\Delta_3 q$ with an interval of 2 mm, and the dashed lines are the contours of 1 mm of hourly rainfall two hours later, copied from Fig. 3. As explained in section 3, the front edge of the 1 mm contours of hourly rainfall can be regarded as the location of the squall line. The two types of contours are collated well at all the times in the series of six hours. The results suggest that the "+2 mm" contours of $\Delta_3 q$ can be used to predict well the location of the squall line two hours later.

An interesting fact is found in the PWV data assimilation experiments with 3D-VAR assimilation. Figure 8 shows the difference between the wind fields with and without the PWV data assimilation at the 850 hPa level at 0800 LST 24 August. The wind vector difference field happened to be a cyclonic wind field, and furthermore the wind velocity reduces towards the

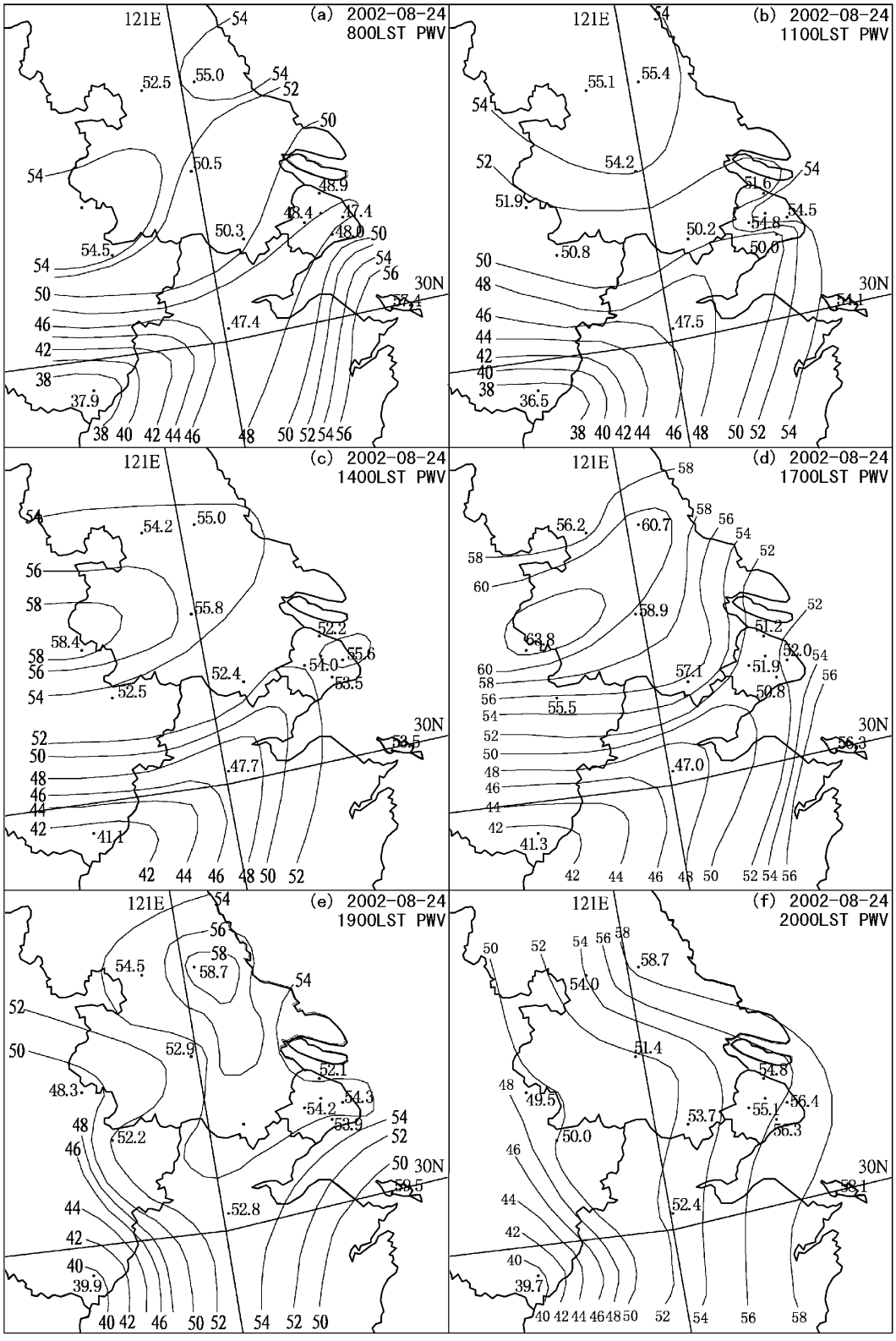

Fig. 6. Evolution of the spatial distribution of PWV in the squall line process in the Yangtze River Delta.

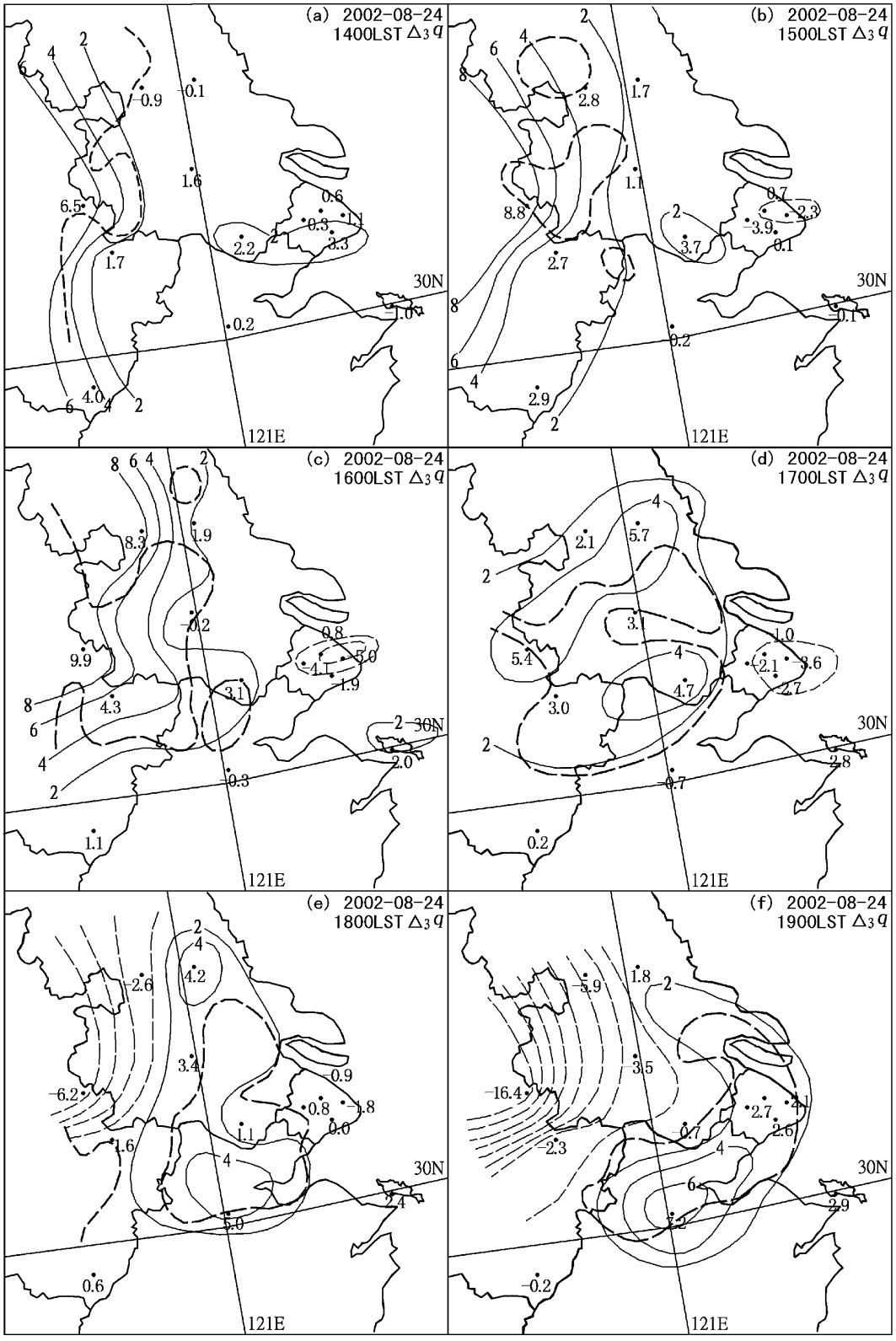

Fig. 7. Corresponding relationship between the variation of PWV and the location of the squall line. Solid lines are the contours of the positive $\Delta_3 q$ with an interval of 2 mm, and the dashed lines are the 1 mm contours of hourly rainfall two hours later, copied from Fig. 3. Times are shown at the upper right corner on each of the panels.

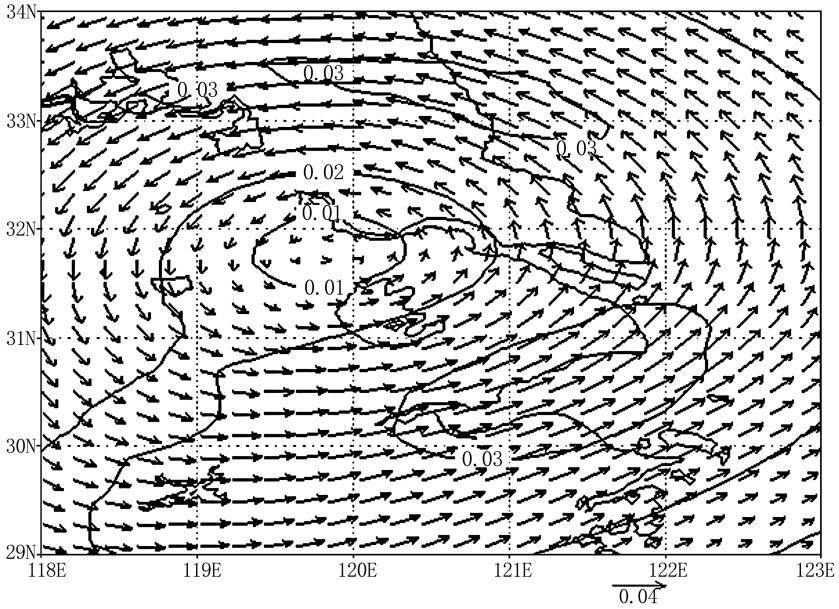

Fig. 8. Differences between the wind fields at the 850 hPa level at 0800 LST 24 August with and without the assimilation of GPS-PWV data.

center. this is favorable to convergence and the ascent of air in the lower level. Because there are only four operational radiosonde stations in the Yangtze River Delta, moisture observations from soundings are not enough to describe the mesoscale structure of the moisture distribution. The assimilation of the GPS-PWV data at 14 stations not only gives a realistic moisture structure, but also made a more favorable wind field for a squall line to form and develop.

6. Conclusions

(1) The squall line swept through the Yangtze River Delta and the rain area expanded and intensified as the squall line moved eastward. The front edge of the contours of 1 mm hourly rainfall coincided basically with the location of the squall line.

(2) Twelve hours prior to the arrival of the squall line, the PWV at a station increased significantly in two stages, providing a favorable moist environment for the squall line to form and develop. Moisture increased mainly in the middle levels rather than at the ground. The temporal variation of the PWV better reflects the squall line approach than surface meteorological parameters do.

(3) The PWV increases in the two different stages are related closely to the evolution of the wind profiles. In the first stage, where the moisture increase at lower levels contributed mainly to the PWV increasing, the prevailing southwest wind in the lower levels brought abundant moisture and made the absolute moisture at the surface increase significantly and the lower layer become wet over the Shanghai area. The northwest wind prevailing in the middle levels brought dry and cold air currents and penetrated over the Shanghai area. The unstable stratification encouraged the development of convection and transferred the moisture upward, making the top of the lower wet layer increase from 1500–3000 m high. The PWV increased mainly due to the moisture supply by the southwest current at lower levels, and the lower wet layer was getting thicker due to the convection. In the second stage, the moisture increase in the middle levels contributed to the PWV increase more than that at the lower levels. The winds in the lower levels changed to northwest or west winds, while in the middle levels the southwest wind changed to be prevailing and brought abundant moisture.

(4) The PWV distribution provided a favorable environment for a squall line to form and develop. The assimilation of the GPS-PWV data at 14 stations not only gave a realistic moisture structure, but also produced a more favorable wind field for a squall line to form and develop.

(5) The "+2 mm" contours of the three-hour PWV variation can be used to predict the location of the squall line two hours later.

Acknowledgements. The work is supported by the Chinese Meteorological Administration (Grant No. CMATG2007M16) and the Ministry of Science and Technology of the People' s Republic of China 863 program

(Grant No. 2006AA12A107). Miss Xi Hong helped to make and optimize the figures in this paper. This paper is supported by the Knowledge Innovation Program of the Chinese Academy of Sciences (KJCX2-SW-T1-3), and the project (Grant No. 032512029) from the Shanghai Scientific Committee of Shanghai Government in China.

REFERENCES

Betts, A. K., 1986: A new convective adjustment scheme. Part I: Observational and theoretical basis. *Quart. J. Roy. Meteor. Soc.*, **112**, 677–692.

Betts, A. K., and M. J. Miller, 1986: A new convective adjustment scheme. Part II: Singlecolumn tests using GATE wave, BOMEX, ATEX and Arctic air-mass data sets. *Quart. J. Roy. Meteor. Soc.*, **112**, 693–709.

Betts, A. K., and M. J. Miller, 1993: The Betts-Miller scheme. The representation of cumulus convection in numerical models, *Meteor. Monogr.*, Amer. Meteor. Soc., **46**, 107–121.

Bi, Y.-M., 2006: Preliminary Results of 4-D Water Vapor Tomography in the Troposphere Using GPS. *Adv. Atmos. Sci.*, **23**(4), 551–560.

Bevis, M., S. Businger, T. A. Herring, C. Rocken, R. A. Anthes, and R. H. Ware, 1992: GPS meteorology: Remote sensing of atmospheric water vapor using the Global Positioning System. *J. Geophys. Res.*, **97**, 787–801.

Bevis, M., S. Businger, S. R. Chiswell, T. A. Herring, R. A. Anthes, C. Rocken, and R. H. Ware, 1994: GPS meteorology: Mapping zenith wet delays onto precipitable water. *J. Appl. Meteor.*, **33**, 379–386.

Businger, S., and Coauthors, 1996: The promise of GPS in atmospheric monitoring. *Bull. Amer. Meteor. Soc.*, **77**(1), 5–18.

Dudhia, J., 1995: Reply to comment on "A nonhydrostatic version of the Penn State/NCAR mesoscale model: Validation tests and simulations of an Atlantic cyclone and cold front" by J. Steppeler. *Mon. Wea. Rev.*, **123**, 2573—2575.

Grell, G. A., J. Dudhia and D. R. Stanffer, 1993: A description of the fifth-generation Penn state/NCAR Mesoscale Model (MM5), NCAR Technical Note, NCAR/TN-398+STR, 120pp.

Kuo, Y.-H., Y.-R. Guo, and E. R. Westwater, 1993: Assimilation of precipitable water vapor into mesoscale numerical model. *Mon. Wea. Rev.*, **121**, 1215–1238.

Kuo, Y.-H., X. Zou, and Y.-R. Guo, 1996: Variational assimilation of precipitable water using a nonhydrostatic mesoscale adjoint model. *Mon. Wea. Rev.*, **124**, 122–147.

MacDonald, A. E., and Y.-F. Xie, 2002: Diagnosis of Three-Dimensional Water Vapor Using a GPS Network. *Mon. Wea. Rev.*, **130**, 386–397.

Qi Liangbo, and Chen Yonglin, 2004: An analysis of a squall line in the Yangtze River area. *Journal of Applied Meteorological Science*, **15**(2), 162–173. (in Chinese)

Shou Shaowen, 2002: *Synoptic Meteorological Analysis 1*. China Meteorological Press, Beijing, 168–169. (in Chinese)

The Meteorological Speciality of the Geophysical Department of Beijing University, 1976: *Synoptic Analysis and Forecast*. Science Press, Beijing, 455–456. (in Chinese)

Yuan Zhaohong, Ding Jincai, and Chen Yonglin, 2004a: A comparison study of precipitable water simulated by NWP and GPS observations. *Chinese J. Atmos. Sci.*, **28**(3), 433–440. (in Chinese)

Yuan Zhaohong, Ding Jincai, and Chen Min, 2004b: Preliminary study on applying GPS observations to mesoscale numerical weather prediction model. *Acta Meteorological Sinica*, **62**(2), 200–212. (in Chinese)

Zhang Peichang, Du bingyu, and Dai Tipei, 2001: *Radar Meteorology*. China Meteorological Press, Beijing, 234–238. (in Chinese)